Electronic Supplementary Material (ESI) for Chemical Communications.

Supramolecular Synthon Approach to Design Amorphous Solid Dispersions with Exceptional Physical Stability

Naga Kiran Duggirala,[†] Jinghan Li,[†] N. S. Krishna Kumar[†] Tata Gopinath[‡] and Raj Suryanarayanan*[†]

[†]Department of Pharmaceutics, College of Pharmacy, University of Minnesota, Minneapolis, MN-55455, United States

[‡]Department of Biochemistry, Molecular Biology, and Biophysics, University of Minnesota, Minneapolis, MN-55455, United States

Materials and methods

Materials. Pyrimethamine (PYR, spectrum), trimethoprim (TMP, TCI), lamotrigine (LAM, Struchem Co., Ltd), polyacrylic acid (PAA, Sigma Aldrich), acrylic acid (ACR, sigma), maleic acid (MLE, Sigma), and acetic acid (ACA, Sigma) were used as received.

Preparation of Amorphous Solid Dispersions. PAA and PYR, were dissolved in methanol. The solvent was evaporated using a rotary evaporator. The solid samples were dried under vacuum for 20-24 hours at RT. A similar procedure was used to make ASDs of TMP and LAM.

X-ray Powder Diffractometry. Data was collected in a diffractometer (model D8 ADVANCE; Bruker AXS, Madison, WI) using Cu K_α radiation (40 kV × 40 mA) over an angular range of 5−35° 2θ with a step size of 0.02° and a dwell time of 0.5 s. The instrument was equipped with a variable-temperature stage (TTK 450; Anton Paar, GrazStraßgang, Austria) and a silicon strip one-dimensional detector (LynxEye, Bruker AXS, Madison, WI, USA). For the variable temperature experiment, the sample was heated at 10 °C/min to 200 °C and the XRD patterns were collected at 10 °C intervals**.**

Physical Mixtures. Samples were prepared by geometric mixing of PAA with each drug in a 35:65 w/w ratio.

IR Spectroscopy. The IR spectra of model drugs, polyacrylic acid and amorphous solid dispersions were obtained in a spectrometer (Vertex 70, Bruker, Ettlingen, Germany; equipped with a globar mid-IR source) using an attenuated total reflectance (ATR) accessory (single reflection germanium crystal) and a DLaTGS detector. The resolution was 4 cm^{-1}, and 64 scans were acquired in the range of 4000–400 cm^{-1}. The peak positions were determined using OPUS software peak picking function.

Differential Scanning Calorimetry. A differential scanning calorimeter (Q2000, TA Instruments, New Castle, DE) equipped with a refrigerated cooling accessory was used. Dry

nitrogen was purged at 50 mL/min. Approximately, 2-5 mg of solid samples were weighed in an aluminum pan, sealed hermetically, heated to the desired temperature at 10°C/min.

Thermogravimetric Analysis. The samples were heated at 10 °C/min under nitrogen purge (50 mL/min) from RT to 300 °C (TGA Q50, TA Instruments, DE, USA). The residual solvent content was determined based on the % weight loss during heating.

Hot-Stage Microscopy. Phase changes were observed using a polarized light microscope (Eclipse e200; Nikon, Tokyo, Japan) equipped with a DS-Fi1 microscope digital camera for capturing digital images. The heating rate was 10 °C/min. The images of PYRPAA were collected up to 250 °C.

Dielectric Analysis. The molecular mobility was measured using a dielectric spectrometer (Novocontrol Alpha AK high performance frequency analyzer, Novocontrol technologies, Germany) at fixed temperatures over a frequency range of 10^{-2} to 10^{7} Hz. The temperature range of dielectric measurements are chosen to cover the supercooled state of the amorphous systems. The powder samples were tightly packed between two gold plated copper electrodes (20 mm diameter) confined by a polytetrafluoroethylene spacer (1 mm thickness, 60 mm^2 area). The calculated free space capacitance was 2.3 pF. Obtained complex dielectric data were analyzed with Eq. 1, using WinFit software from Novocontrol.

$$\varepsilon^*(\omega) = \varepsilon''(\omega) - i\varepsilon''(\omega) = \varepsilon_\infty + \frac{\Delta\varepsilon}{(1 + (i\omega\tau_{HN})^\alpha)^\gamma} + \frac{\sigma_0}{i\omega\varepsilon_0} + A\omega^{-n} \quad \text{---------- (1)}$$

In Equation (1), ω is the angular frequency, ε'(ω) is the real part and ε"(ω) is the imaginary part of the permittivity, ε_∞ is the high frequency dielectric constant, σ_0 is the dc conductivity. The electrode polarization contribution to the real part of the dielectric constant is considered as a power law dependence, $A\omega^{-n}$ (first order approximation), where A is the strength parameter and n is the exponent. The α-relaxation process is modelled with the Havriliak-Negami (HN) function, where Δε is the dielectric strength of the α-relaxation process, τ_{HN} is the HN relaxation time and, α and γ are the shape parameters which determine respectively the symmetric and asymmetric broadening of dielectric loss peak. The fit parameters were obtained using Eq. (1). The dielectric relaxation time (τ) was determined from peak maximum of dielectric loss peak with HN parameters using Eq. (2).

$$\tau = \tau_{HN}\left[sin\left(\frac{\alpha\Pi}{2+2\gamma}\right)\right]^{-1/\alpha}\left[sin\left(\frac{\alpha\gamma\Pi}{2+2\gamma}\right)\right]^{1/\alpha} \quad \text{----------(2)}$$

ε'(ω) data of LAMPAA ASD, at different temperatures, were fitted using Eq. 1 and shown in Fig S13.

Nuclear Magnetic Resonance Spectroscopy. Solid-state NMR spectra were acquired at the Minnesota NMR Center using a Bruker spectrometer operating at a 1H Larmor frequency of 700 MHz and equipped with 3.2 mm MAS probe. All the spectra were acquired at 25 °C using the Hartmann-Hahn cross polarization (CP) experiment at 12 kHz MAS rate.[1] The CP contact time was set to 3 ms for all the samples. A comparison of peak intensities at different CP contact times was performed on PYR samples. The recycle delay was set to 3 s, and 15N acquisition time was set to 10 ms with 100 kHz spectral width. During CP, 15N and 1H RF amplitudes were set to 35 and 59 kHz respectively. SPINAL decoupling was used during acquisition with 83.33 kHz 1H RF amplitude.[2] A total of 15,000 to 35,000 scans were used for acquiring each sample.

Single Crystal X-ray Crystallography. A crystal (approximate dimensions 0.200 x 0.150 x 0.140 mm^3) was placed onto the tip of a 0.1 mm diameter Mitegen loop and mounted on a Bruker PHOTON-II diffractometer for a data collection at 100(2) K.[3] A preliminary set of cell constants was calculated from reflections harvested from two sets of frames. These initial sets of frames were oriented such that orthogonal wedges of reciprocal space were surveyed. This produced an initial orientation matrix determined from 367 reflections. The data collection was carried out using MoKα radiation (parabolic mirrors) with a frame time of 8 seconds and a detector distance of 5.0 cm. A strategy program was used to assure complete coverage of all unique data to a resolution of 0.70 Å. All major sections of frames were collected with 1.20º steps in ω or ϕ at different detector positions in 2θ. The intensity data were corrected for absorption and decay (SADABS).[4] Final cell constants were calculated from 2998 strong reflections from the actual data collection after integration (SAINT).[5] Please refer to Table S2 for additional crystal and refinement information.

Dissolution Studies. A USP apparatus 2 (Varian 705 DS, Agilent Technologies, Santa Clara, CA; paddle speed 100 rpm) was used. All the ASDs were passed through US # 80 mesh and a weighed amount of sample was dispersed in 500 mL of medium (pH 6.8) set at 37 °C. Three mL aliquots were withdrawn at defined time points, filtered (0.45 μm syringe) and analyzed using a UV-Visible spectrophotometer (Cary 100 UV-Vis, Agilent Technologies).

Scanning Electron Microscopy with Energy Dispersive X-ray Spectrophotometry.
A field emission gun scanning electron microscope (FEG-SEM), JEOL 6500 equipped with an energy dispersive spectrometer (EDS) was used for morphological analyses. It has an operating range of 0.5 to 30 kV with an ultimate resolution of 1.5 nm. Secondary electron imaging was

used for the mapping. The powder samples were mounted on an aluminum stub using a double-sided adhesive carbon tape and coated with a thin layer (30 nm) of carbon.

Cambridge Structural Database Analysis

The supramolecular synthon formation of carboxylate/carboxylic acid and 2-amino aromatic nitrogen, specifically for the model drugs PYR, TMP, and LAM, was analyzed using CSD (version 5.39). The analysis was conducted as follows: (i) the total number of structures containing both carboxylic acid and one of the model drugs (PYR, TMP, and LAM); (ii) the number of structures that form a supramolecular heterosynthon between carboxylic acid/carboxylate moieties and 2-amino aromatic nitrogen; (iii) the occurrence of supramolecular heterosynthon for carboxylate and 2-amino aromatic nitrogen; (iv) number of structures where the protonation of the most basic nitrogen occurred in the drug molecule.

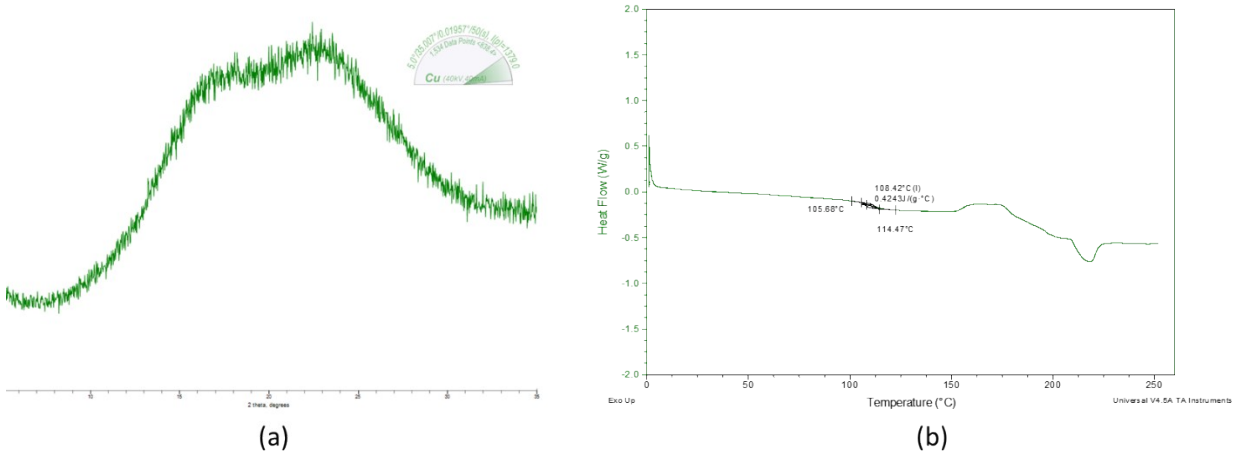

Figure S1. (a) Powder X-ray diffraction (PXRD) pattern, and (b) Differential scanning calorimetry (DSC) heating curve of PYRPAA.

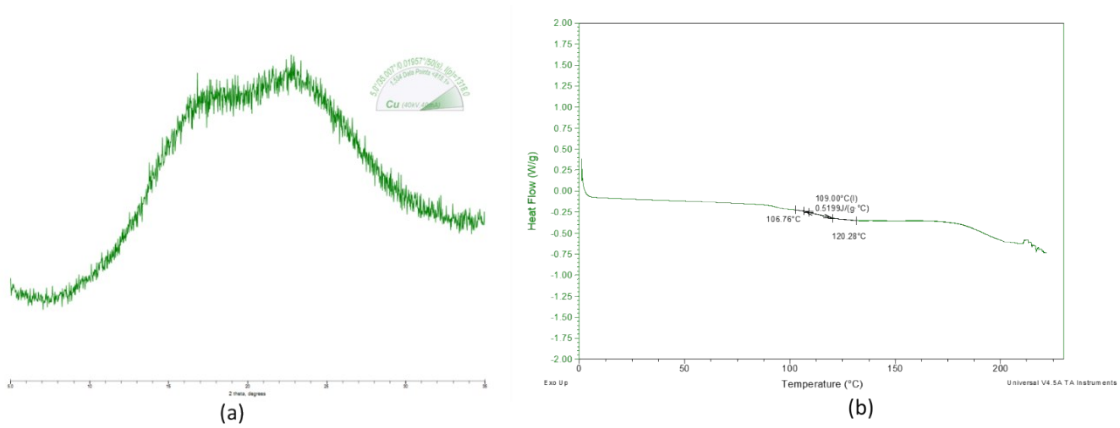

Figure S2. (a) PXRD pattern, and (b) DSC curve of TMPPAA.

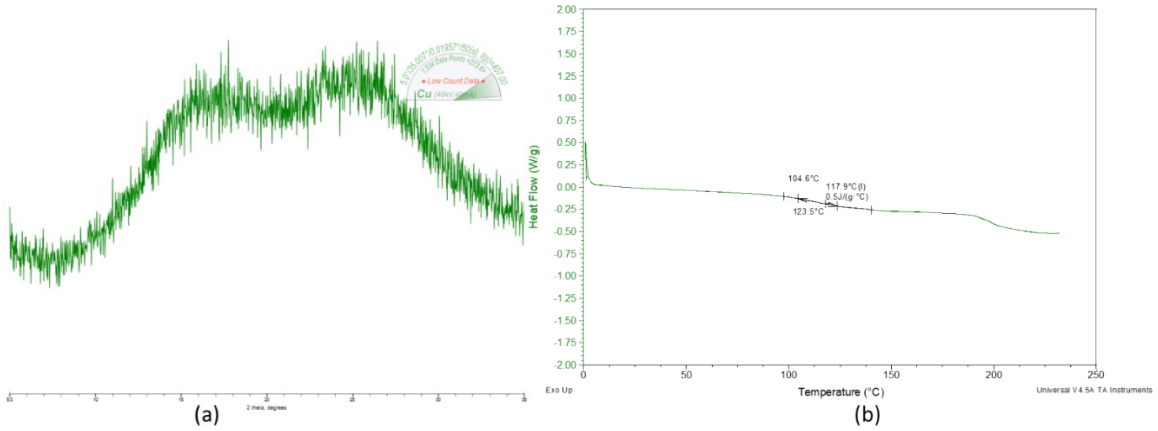

Figure S3. (a) PXRD pattern, and (b) DSC curve of LAMPAA.

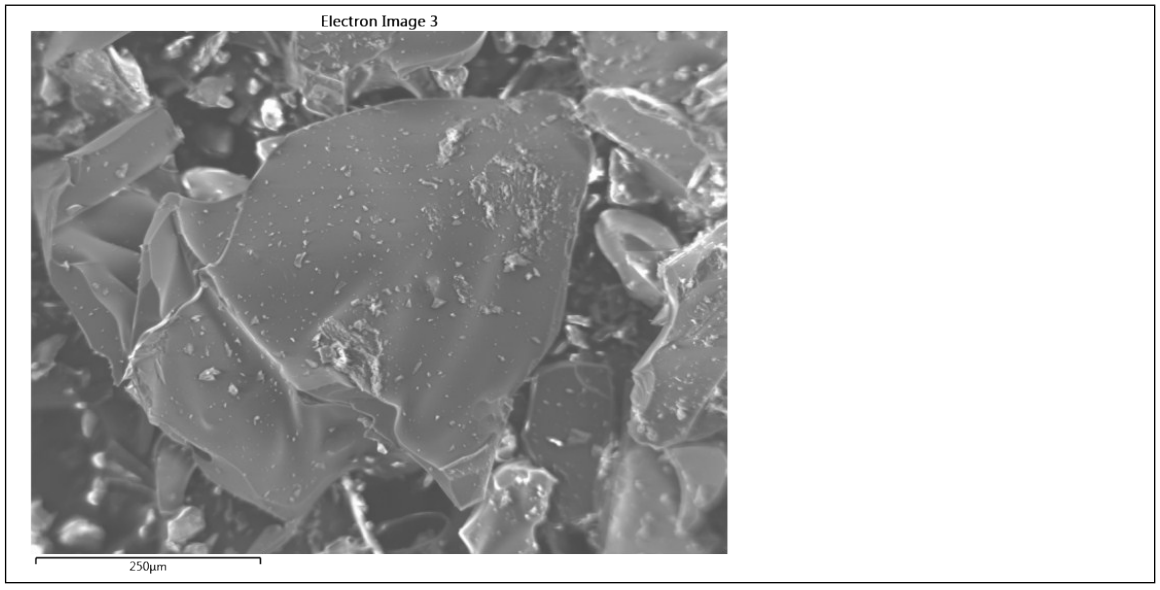

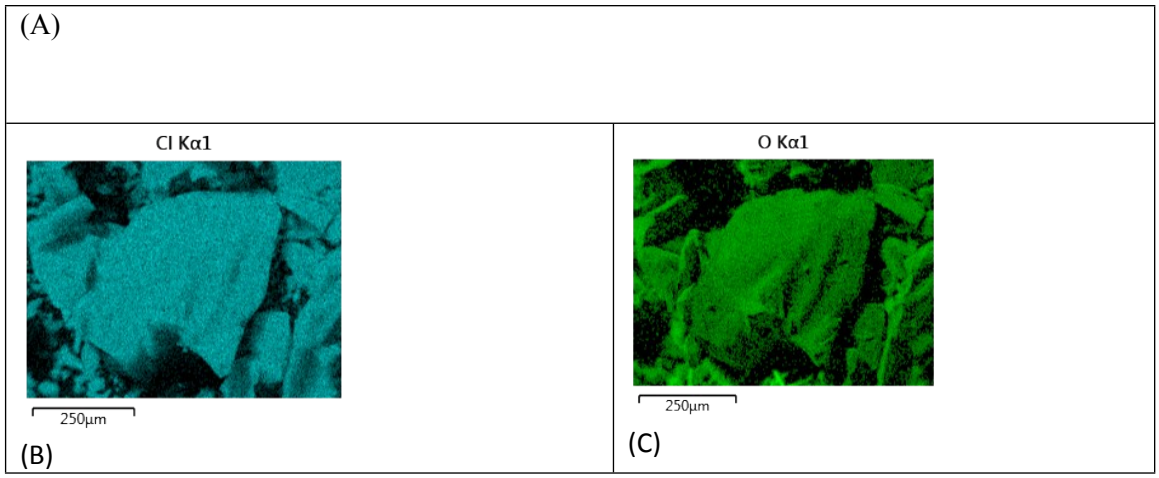

Figure S4. (A) Scanning electron microscope (SEM) image of PYRPAA. (B) Energy dispersive spectrometric (EDS) maps of (B) chlorine and (C) oxygen.

The chlorine atom was used as a "marker" of the drug in the ASDs while oxygen was used as a marker of polymers. This was done since PYR contains chlorine but not oxygen, while PAA contains oxygen but not chlorine.

EDS revealed a homogeneous distribution of chlorine (panel B) and oxygen (panel C) over the surface of PYRPAA.

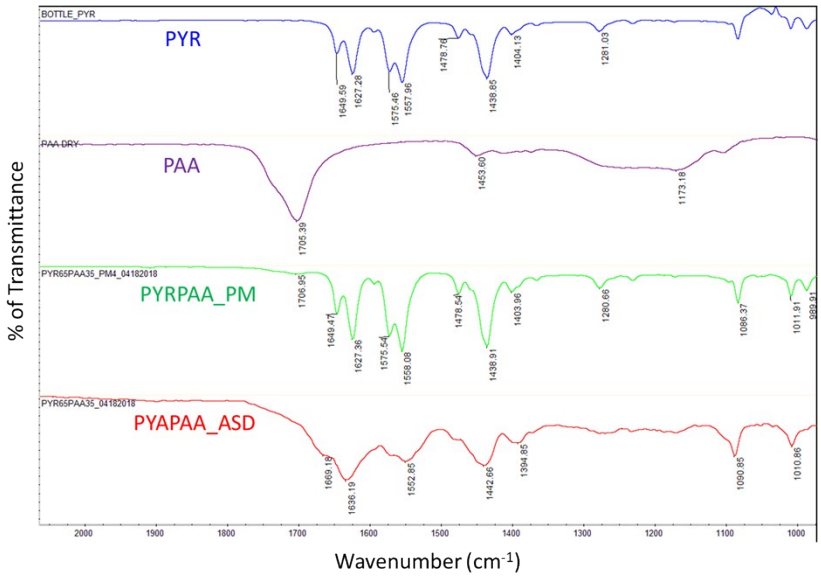

Figure S5. IR spectra of neat PYR, PAA, physical mixture of PYR+PAA, and PYRPAA ASD over a range of 1000-2000 cm^{-1}.

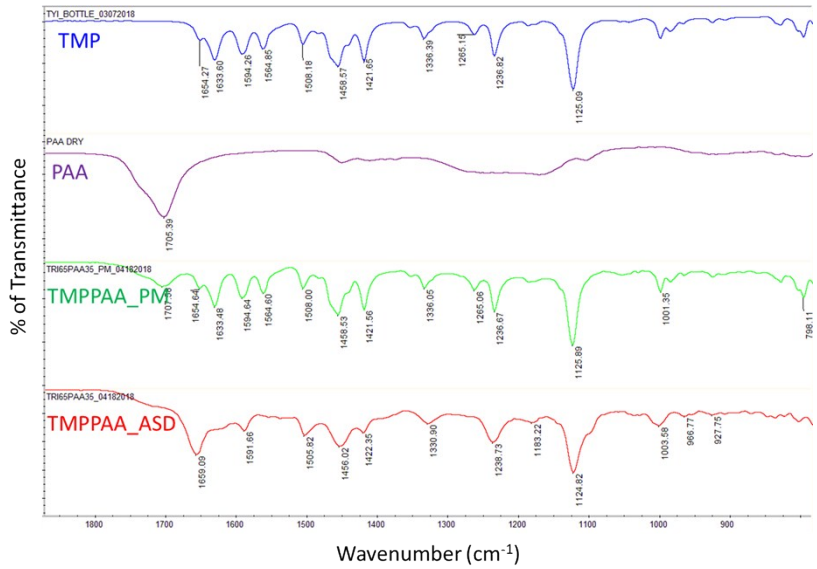

Figure S6. IR spectra of neat TMP, PAA, physical mixture of TMP+PAA, and TMPPAA ASD over a range of 900-1900 cm^{-1}.

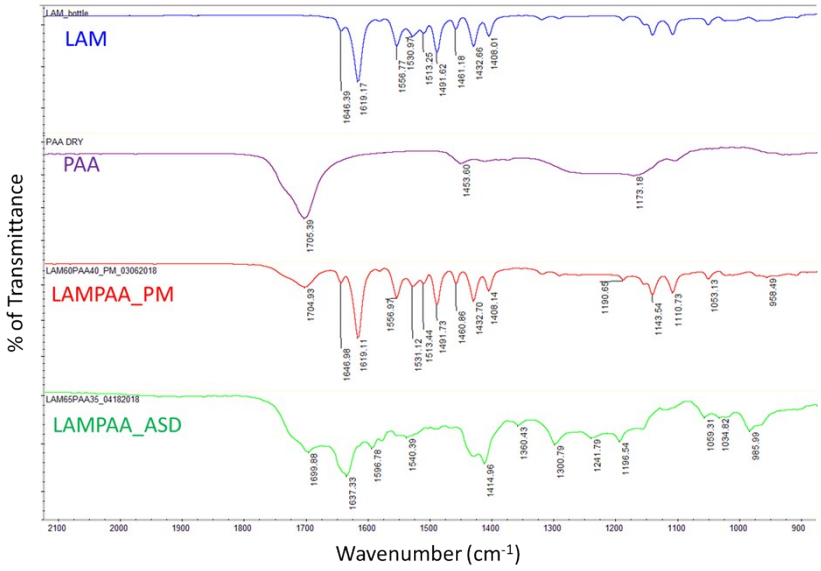

Figure S7. IR spectra of neat LAM, PAA, physical mixture of LAM+PAA, and LAMPAA ASD over a range of 900-2100 cm^{-1}.

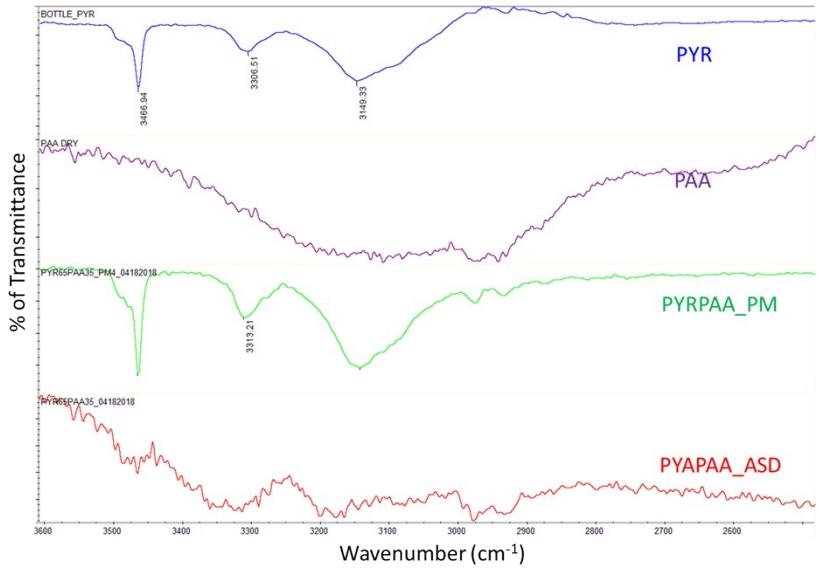

Figure S8. IR spectra of neat PYR, PAA, physical mixture of PYR+PAA, and PYRPAA ASD over a range of 2600-3600 cm^{-1}.

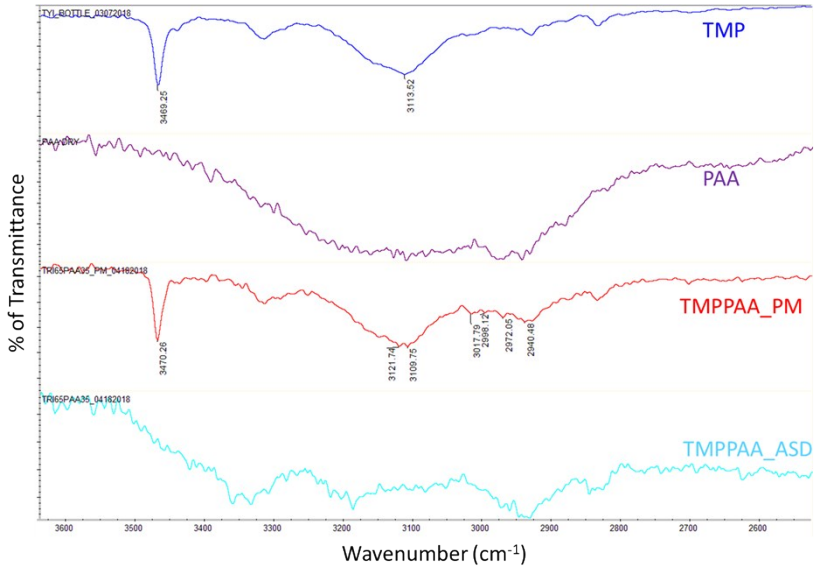

Figure S9. IR spectra of neat TMP, PAA, physical mixture of TMP+PAA, and TMPPAA ASD over a range of 2600-3600 cm^{-1}.

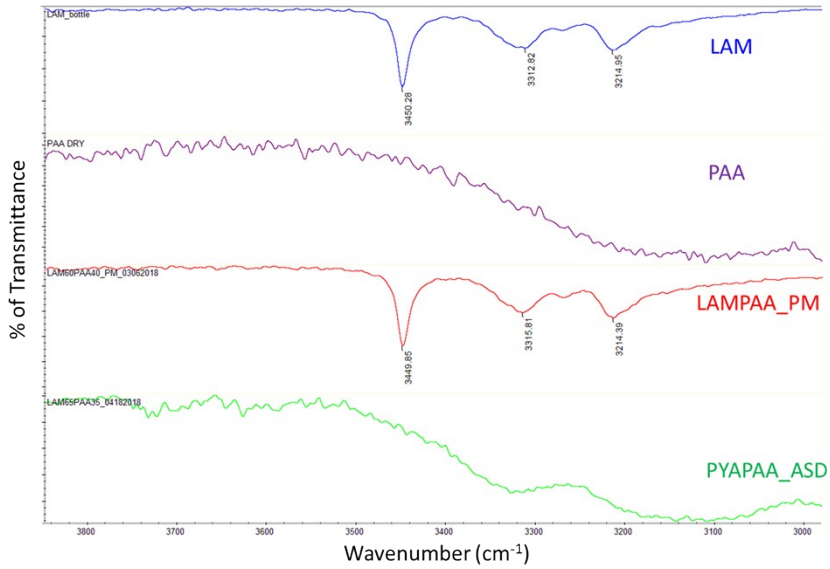

Figure S10. IR spectra of neat LAM, PAA, physical mixture of LAM+PAA, and LAMPAA ASD over a range of 3000-3800 cm^{-1}.

Table S1. Calculation of number of drug molecules "available" per monomer unit of the polymer for the ionic interaction.

Drug	Molecular Weight (g/mol)	Drug to monomer ratio (w/w)				
		10% w/w	20% w/w	30% w/w	40% w/w	50% w/w
TMP	290.32	~4.6:1	~2.0:1	~1.2:1	~0.75:1	~0.5:1
LAM	256.09	~5.2:1	~2.3:1	~1.3:1	~0.86:1	~0.6:1
PYR	248.71	~5.2:1	~2.3:1	~1.3:1	~0.86:1	~0.6:1

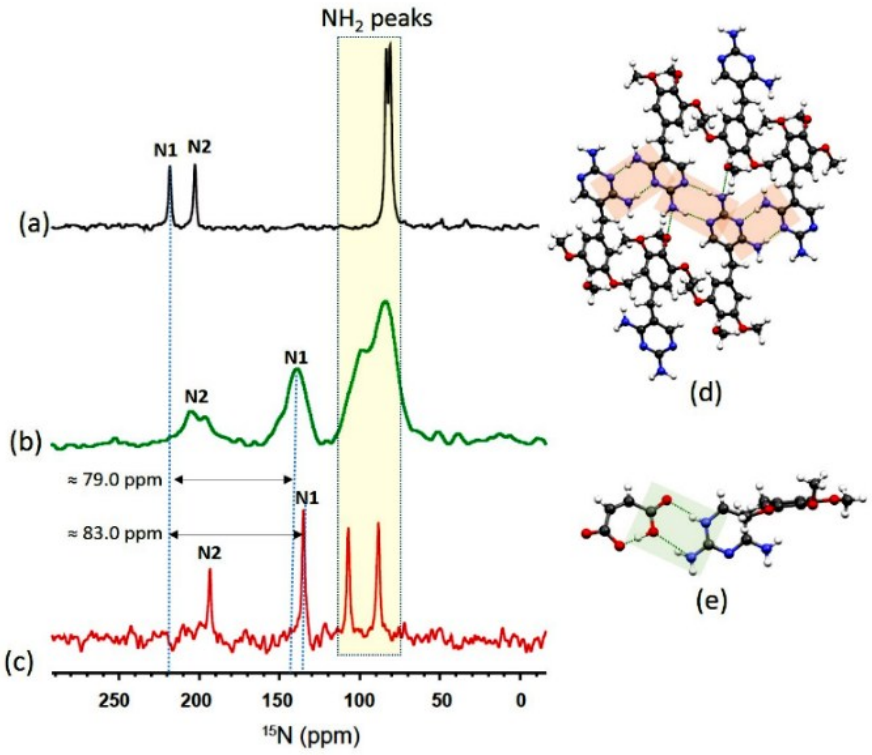

Figure S11. ^{15}N solid-state NMR spectra of (a) TMP (drug); (b) TMPPAA (ASD); and (c) TMPMLE (salt). The illustration of hydrogen bond interactions: (d) supramolecular homo synthon in crystalline TMP, and (e) supramolecular heterosynthon, in TMP hydrogen maleate. The NH_2 peaks [well resolved in crystalline TMP hydrogen maleate (in c)], are broadened in amorphous TMPPAA (b).

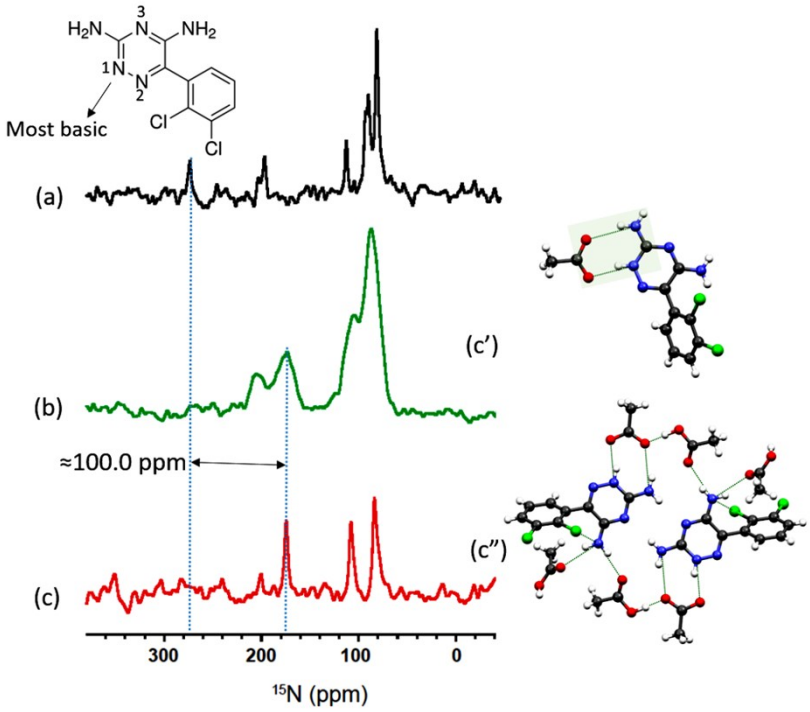

Figure S12. ^{15}N solid-state NMR spectra of (a) LAM (drug); (b) LAMPAA (ASD); and (c) LAMACA (salt). The illustration of hydrogen bond interactions: (C') supramolecular homo synthon in crystalline LAM, and (C'') supramolecular heterosynthon, in LAM acetate-acetic acid.

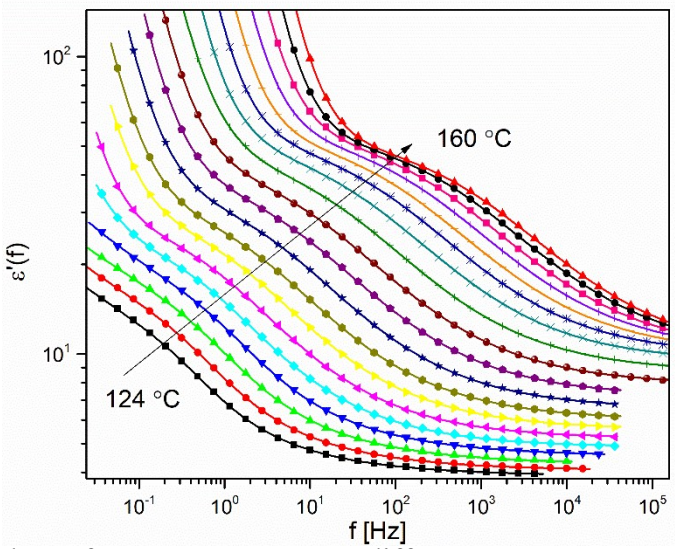

Figure S13. The ε'(ω) data of LAMPAA ASD, at different temperatures, were fitted using Eq. (1).

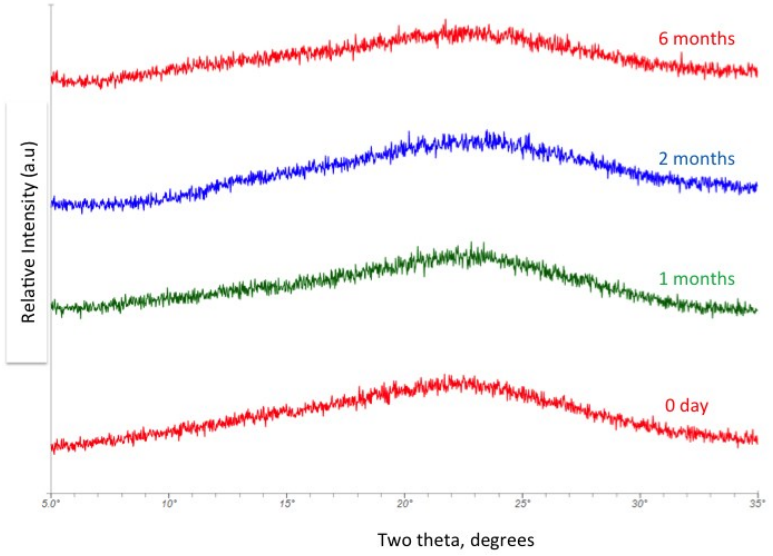
6 months
2 months
1 months
0 day
Relative Intensity (a.u)
5.0°
10°
15°
20°
25°
30°
35°
Two theta, degrees

(a)

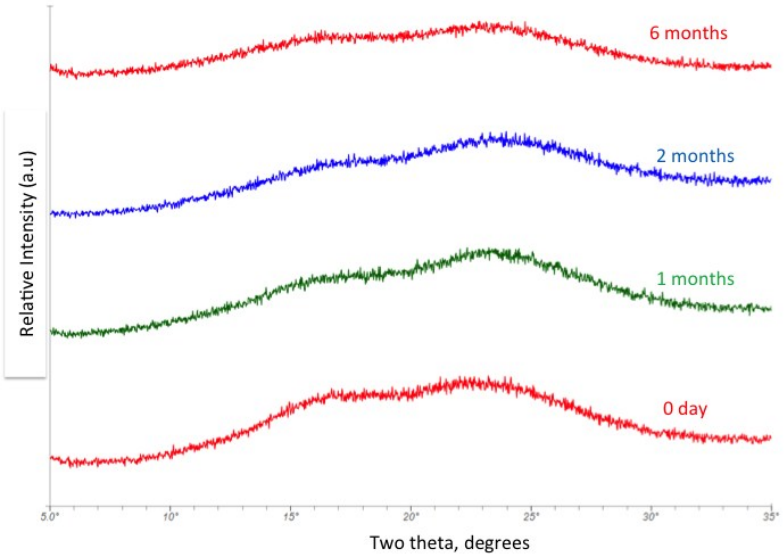
6 months
2 months
1 months
0 day
Relative Intensity (a.u)
5.0°
10°
15°
20°
25°
30°
35°
Two theta, degrees

(b)

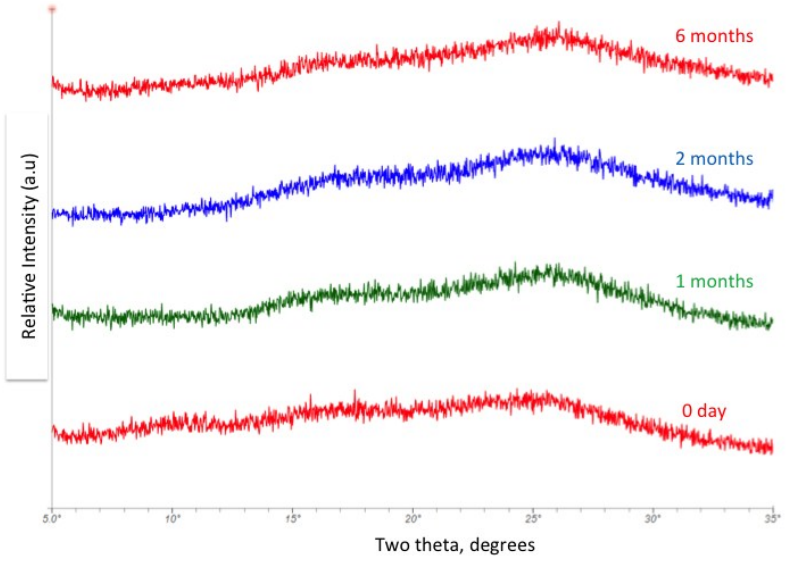

(c)

Figure S14. Overlay of PXRD patterns collected for ASDs of (a) PYRPAA, (b) TMPPAA, and (c) LAMPAA, stored in an open vials at 40 °C/75% RH for up to 6 months.

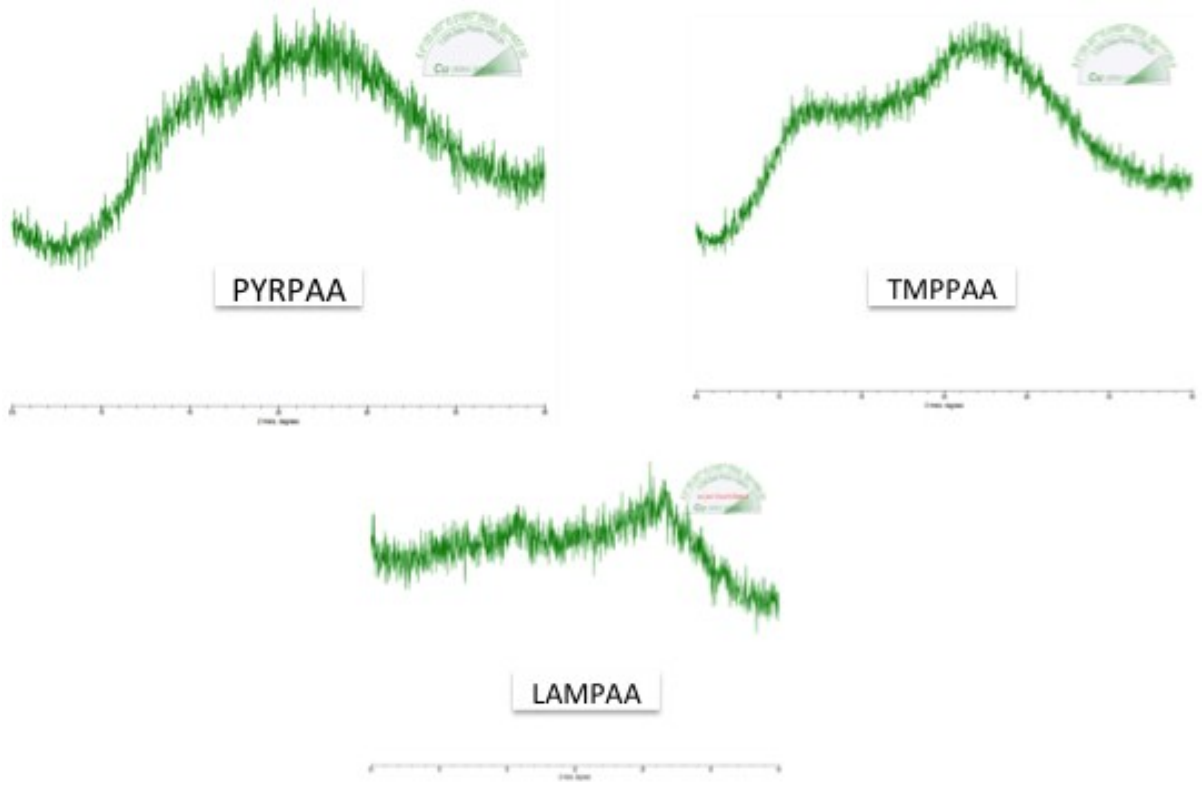

Figure S15. XRD patterns of ASDs, after slurrying in water for 24 hours.

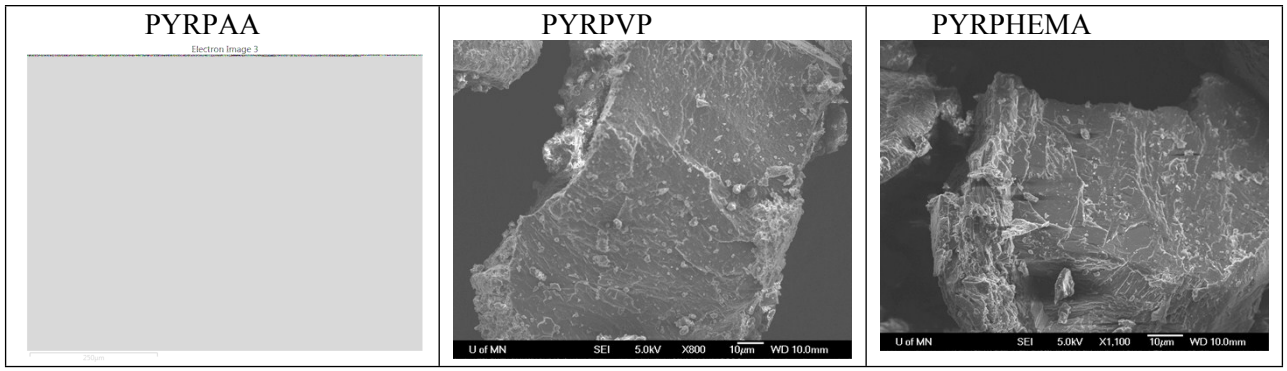

Figure S16. Scanning electron microscope (SEM) images of PYRPAA, PYRPVP and PYRPHEMA. The surface of PYRPAA ASD was relatively smooth whereas irregular shaped morphologies were observed in both PYRPHEMA and PYRPVP.

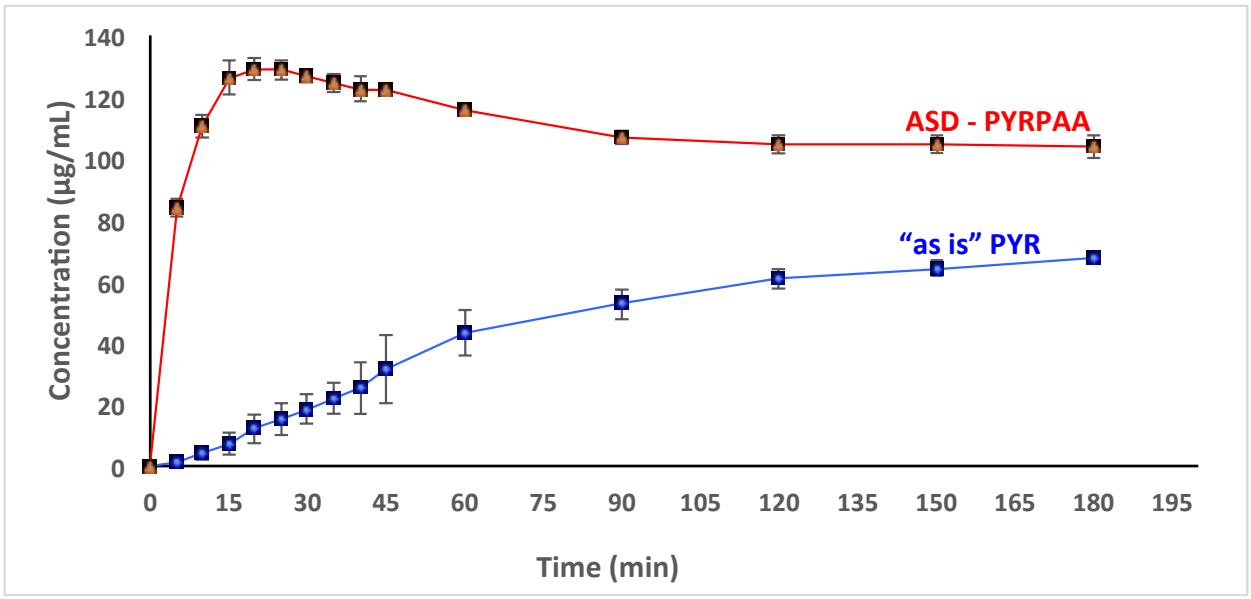

Figure S17. Dissolution profile of "as is" PYR and PYRPAA ASD in phosphate buffer (pH 6.8, 37 °C)

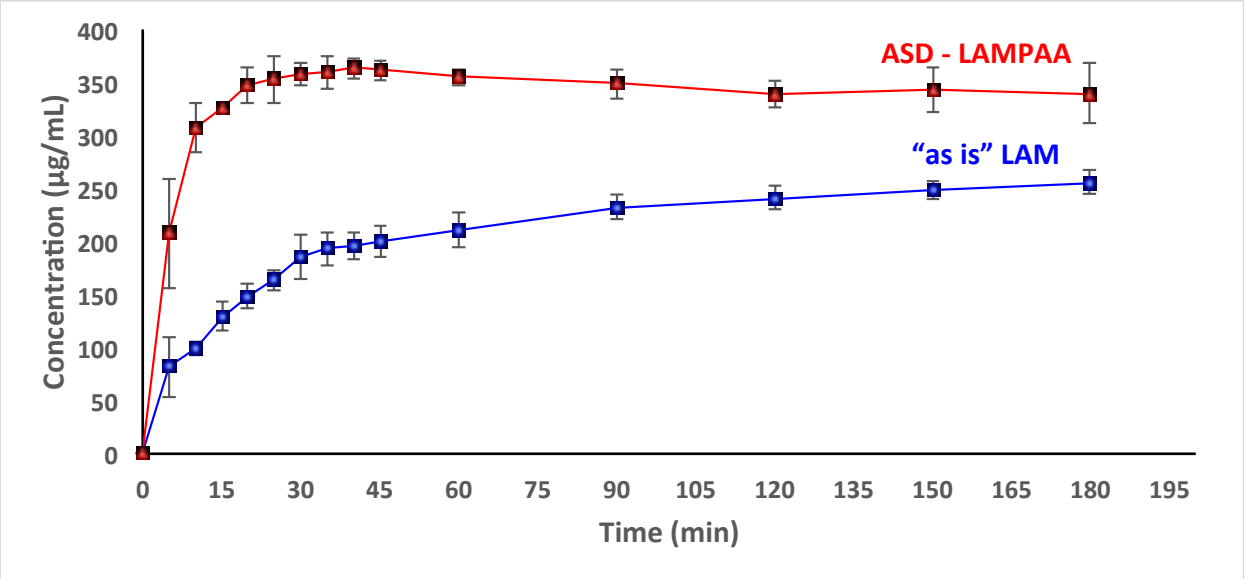

Figure S18. Dissolution profile of "as is" LAM and LAMPAA ASD in phosphate buffer (pH 6.8, 37 °C)

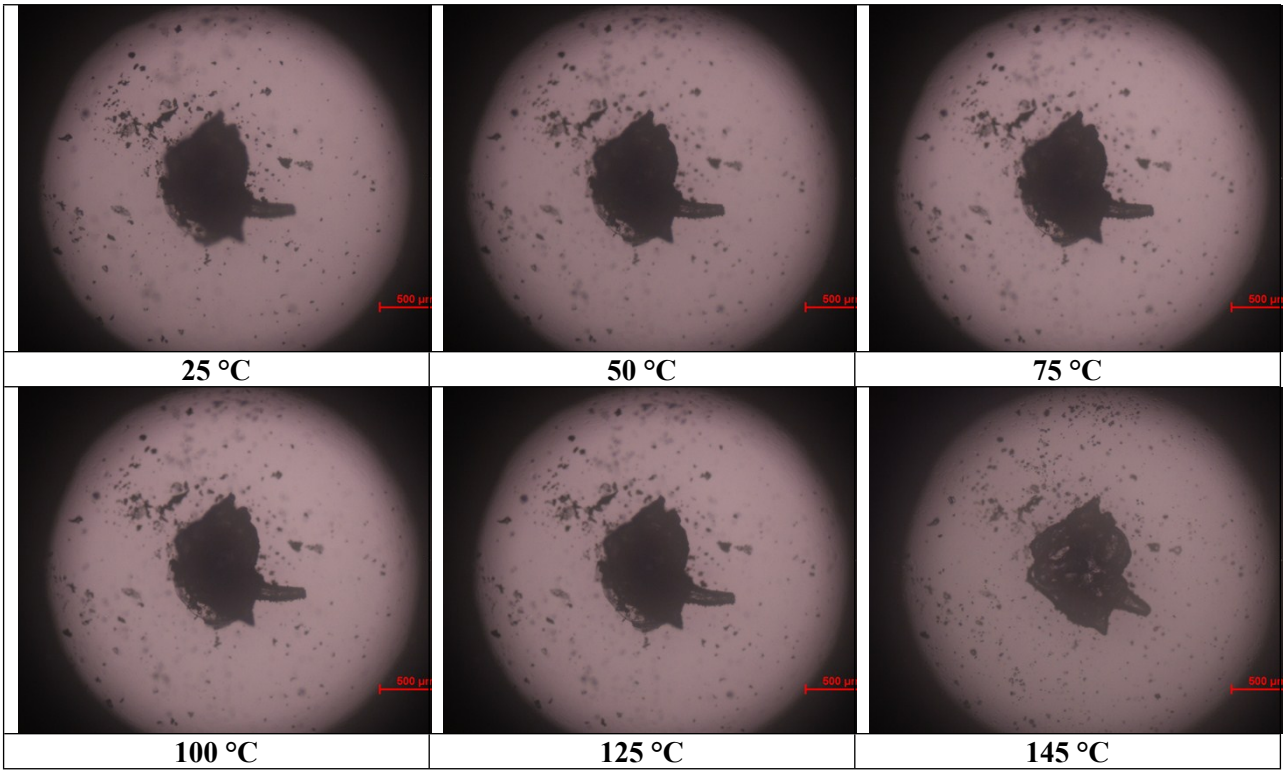

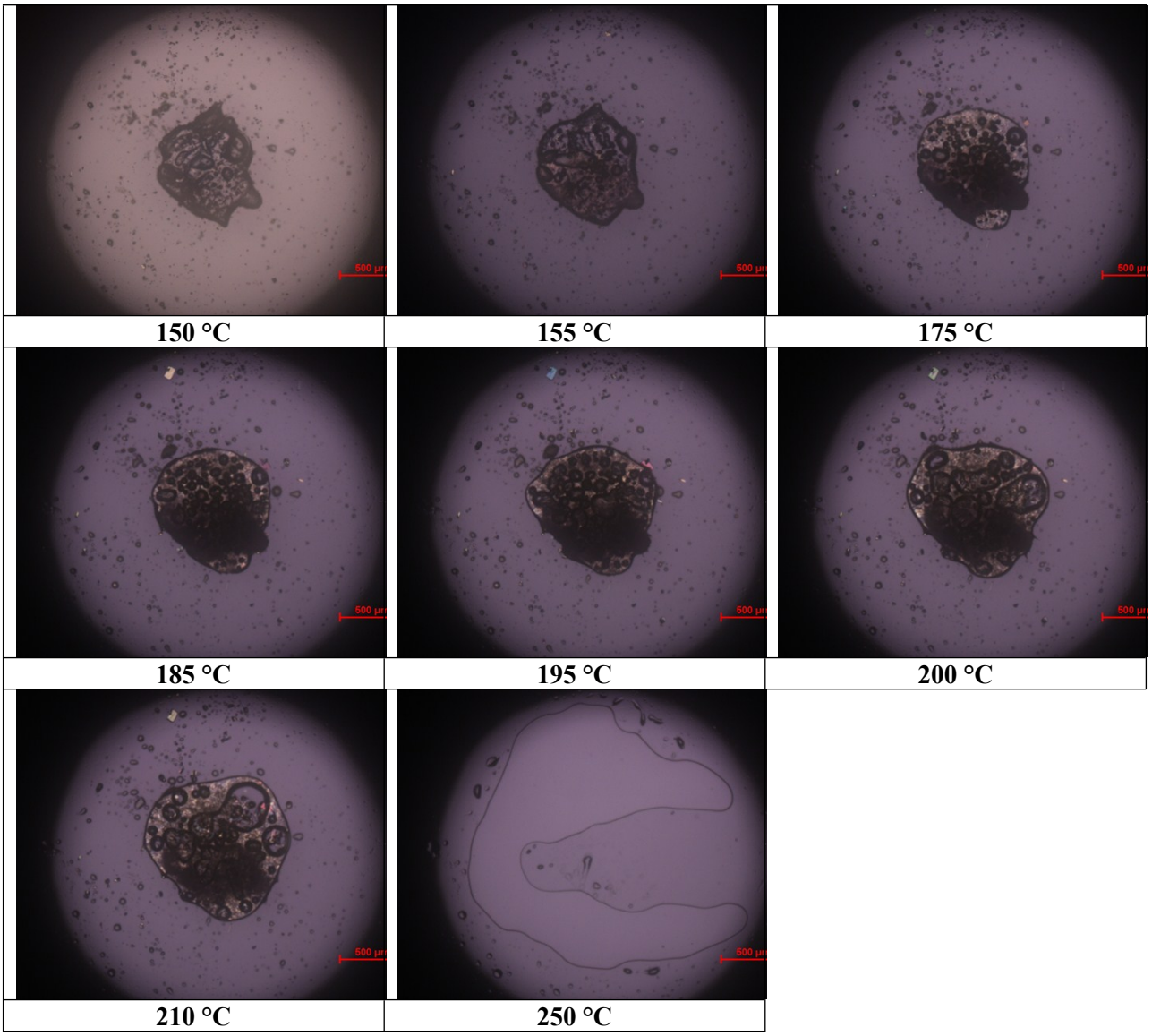

Figure S19. Hot stage microscopic images collected at different temperatures when PYRPAA was subjected to a controlled temperature program in the temperature range of 25-250 °C; crystallization of PYR is evident and is in good agreement with the exotherm observed in the DSC at ~ 150 °C (Figure S1).

Table S2. The crystal structures along with their REFCODEs, retrieved from CSD that contain pyrimethamine and a carboxylic acid coformer.

CSD Refcode	**Coformer**	**pK_a of carboxylic acid**	**Δ pKa**	**Protonation on N1**
AFESOU	3,5-dinitrobenzoicacid	1.6	5.7	Y
AYUQAN	Acetamido benzoicacid	3.6	3.7	Y
AZOQAI	Propanamido benzoicacid	3.6	3.7	Y
BOJGEN	Picolinic acid	1.0	6.3	Y
GINNIB*	Nicotinic acid	2.0	5.3	Y
KICVOJ*	P-coumaric acid	1.0	6.3	Y
KICVUP*	Aspirin	3.5	3.8	Y
KICWAW	Ketoglutaric acid	2.4	4.9	Y
KUQQUJ	4-methylbenzoicacid	4.3	3.0	Y
KUQRAQ	3-hydroxypicolinic acid	0.4	6.9	Y
KUQREU	2,4 dichlorobenzoic acid	3.6	3.7	Y
LENKEV	3-chlorobenzoic acid	3.8	3.5	Y
PARXAI	2-nitrobenzoic acid	2.2	5.1	Y
PARXEM	3-nitrobezoic acid	3.5	3.8	Y
PARXIQ	4-nitrobezoic acid	3.4	3.9	Y
UHAYEH	Glutaric acid	4.3	3.0	Y
UHAYIL	Formic acid	3.8	3.5	Y
ULAXIO	Fumaric acid	3.0	4.3	Y
ULAXOU	Maleic acid	1.8	5.5	Y
ULAXUA	Phthalic acid	2.9	4.4	Y
ULAYAH	Succinic acid	4.2	3.1	Y
XEGGUN*	Oxalic acid	1.3	6.0	Y
XEGHAU*	Malonic acid	2.8	4.5	Y
XEGHIC01	Adipic acid	4.4	2.9	Y
XEGHOI	Pimelic acid	4.5	2.8	Y
XEGHUO*	Suberic acid	4.5	2.8	Y
XEGJAW*	Azelic acid	4.6	2.7	Y
YALVAK*	Terephthalic acid	3.5	3.8	Y
YALVEO*	Terephthalic acid	3.5	3.8	Y
This study	**Acrylic acid**	**4.2**	**3.1**	**Y**
OBECIJ*	2,6-dioxo-1,2,3,6-tetrahydropyrimidine-4-carboxylic acid	NF	-	Y
XEGHEY	Acetylene dicarboxylic acid	NF	-	Y

JOBSEA*	2-((4-trifluoromethyl)phenylsulfanyl)benzoic acid	NF	-	Y

Y- Protonation on N1; NF – pK_a values were not found; * solvate/hydrate

CSD Analysis of Pyrimethamine

pK_a of Pyrimethamine - 7.3

pK_a range of coformers - 0.4 to 4.6

Overall ΔpK_a range = 6.9 to 2.7

Total number of crystal structures retrieved = 34

Occurrence of protonation of N1 - 100 % (34/34)

Counterion used in the present study: Acrylic acid pK_a = 4.2

ΔpK_a = 3.1

Table S3. The crystal structures along with their REFCODEs, retrieved from CSD that contain Trimethoprim and a carboxylic acid coformer.

CSD Refcode	**Coformer**	**pK_a of carboxylic acid**	**Δ pKa**	**Protonation on N1**
CACBOY	Glutaric acid	4.3	2.3	Y
CESRUN	Benzoic acid	4.2	2.4	Y
CUCSEY01	Benzoic acid	4.2	2.4	Y
CURSAL	Fumaric acid	3.0	3.6	y
FUWVAU	Acetic acid	4.8	1.8	Y
HAMYIE	Malonic acid	2.8	3.8	Y
HEGHIL	Nicotinic acid	2.0	4.6	Y
HURMOW	3-chlorobenzoic acid	3.8	2.8	Y
HURMUC*	3-chlorobenzoic acid	3.8	2.8	Y
KADFUR*	Sorbic acid	4.8	1.8	Y
KADGAY	O-nitrobenzoic acid	2.2	4.4	Y
MIFWUT*	Salicylic acid	3.0	3.6	Y
NATHEW*	Picolinic acid	1.0	5.6	Y
PARWOV	3-nitrobenzoic acid	3.5	3.1	Y
PARWUB	4-nitrobenzoic acid	3.4	3.2	Y

QIKDIX	**Maleic acid**	**1.9**	**4.7**	**Y**
QOVROJ	Malic acid	3.4	3.2	Y
SEMNAA	Phthalic acid	2.9	3.7	Y
SEMNEE	Adipic acid	4.4	2.2	Y
VADVOM	Terephthalic acid	3.5	3.1	Y
VASFUS*	Cinnamic acid	4.4	2.2	Y
WOYPIJ	Trifluoro acetic acid	0.2	6.4	Y
YECNEA	Succinic acid	4.2	2.4	Y
HILPOI	3,5 dinitrobenzoic acid	1.6	4.0	Y

Y- Protonation on N1; NF – pK_a values were not found; * solvate/hydrate

CSD Analysis of Trimethoprim.

pK_a of Trimethoprim – 6.6

pK_a range of coformers – 0.2 to 4.8

Overall ΔpK_a range = 6.4 to 1.8

Total number of crystal structures retrieved = 24

Occurrence of protonation of N1– 100 % (24/24)

Counterion used in the present study: Maleic acid pK_a = 1.9

ΔpK_a = 4.7

Table S4. The crystal structures along with their REFCODEs, retrieved from CSD that contain Lamotrigine and a carboxylic acid coformer.

CSD Refcode	**Coformer**	**pK_a of carboxylic acid**	**Δ pKa**	**Protonation of N1**
VECTOP	Oxalic acid	1.3	4.4	Y
VECTUV*	Malonic acid	2.8	2.9	Y
VECVAD	Sebacic acid	4.7	1.0	Y
FOXLUA02*	Succinic acid	4.2	1.5	Y
FOXMAH*	Succinic acid	4.2	1.5	Y
FUHVOU02*	Fumaric acid	3.0	2.7	Y
GAVLEV*	Benzoic acid	4.2	1.5	Y
HUQVIA	Cinnamic acid	4.4	1.3	N
IWIZAQ	L-malic acid	3.4	2.3	Y
LIBTUN	Propanoic acid	4.9	0.8	Y

LIBXUR*	**Acetic acid**	**4.9**	**0.8**	**Y**
LIBYAY	4-hydroxybenzoic acid	4.5	1.2	Y
NESBAQ*	Adipic acid	4.4	1.3	Y
NESBEU*	Adipic acid	4.4	1.3	Y
NESBIY*	Pimelic acid	4.7	1.0	Y
NESBOE*	Pimelic acid	4.7	1.0	Y
OVUMIC*	Pyridine 3-carboxylic acid	2.0	3.7	Y
PEZKAI*	Glutaric acid	4.3	1.4	Y
PEZKEM*	Sorbic acid	4.8	0.9	Y
PEZKIQ	**Acetic acid**	**4.9**	**0.8**	**Y**
QIQHIJ*	4-iodobenzoic acid	4.0	1.7	Y
QIQHOP*	4-methylbenzoic acid	3.9	1.8	N
SAVWAQ	Crotonic acid	4.7	1.0	Y
SAVWEU*	2-hydroxy benzoicacid	3.0	2.7	Y
SEGGOC	Fumaric acid	3.0	2.7	Y
SEGHAP	Succnic acid	4.2	1.5	Y
SEGHIX*	Succinic acid	4.2	1.5	Y
SEGHOD*	D-tartaric did	2.9	2.8	Y
SEGHUJ*	Tartaric aid	2.9	2.8	Y
SEGJAR*	Tartaric acid	2.9	2.8	Y
SEGJEV*	D-malic acid	3.4	2.3	Y
WOKXIF	2,5 dihydroxy benzoic acid	3.0	2.7	Y
WOKXUR	4-bromobenzoic acid*	4.0	1.7	N
WUVKUU	Adipic acid	4.4	1.3	Y
WUVLAB	L-malic acid	3.4	2.3	Y
WUVLEF01*	Nicotinic acid	2.0	3.7	Y
YEXFUD*	Phthalic acid	2.9	2.8	Y
AYAXOP*	Dithiodobenzoic acid	NF	-	Y
AYAXUV	Dithiodobenzoic acid	NF	-	Y
OVUMEY	Acetylene dicarboxylic acid	NF	-	Y
QIQJAD	3,5 dinitro 2-hydroxybenzoic acid*	NF	-	Y
SEGGES	Acetylene dicarboxylic acid	NF	-	Y
SEGKAS	meso-2,3	NF	-	Y

	dibromosuccinic acid*			
SEGGIW	Acetylene dicarboxylic acid	NF	-	Y

Y- Protonation on N1; NF – pK_a values were not found; * solvate/hydrate

CSD Analysis of Lamotrigine.

pK_a of Lamotrigine - 5.7

pK_a range of coformers - 1.0 to 4.9

Overall ΔpK_a range = 4.7 to 0.8

Total number of crystal structures retrieved = 44

Occurrence of protonation of N1– 100 % (41/44)

Counterion used in the present study: Acetic acid, pK_a = 4.8

ΔpK_a = 0.8

In overall, for the three model compounds, the ΔpK_a with the selected coformers is 0.8 to 4.

Single Crystal Data:

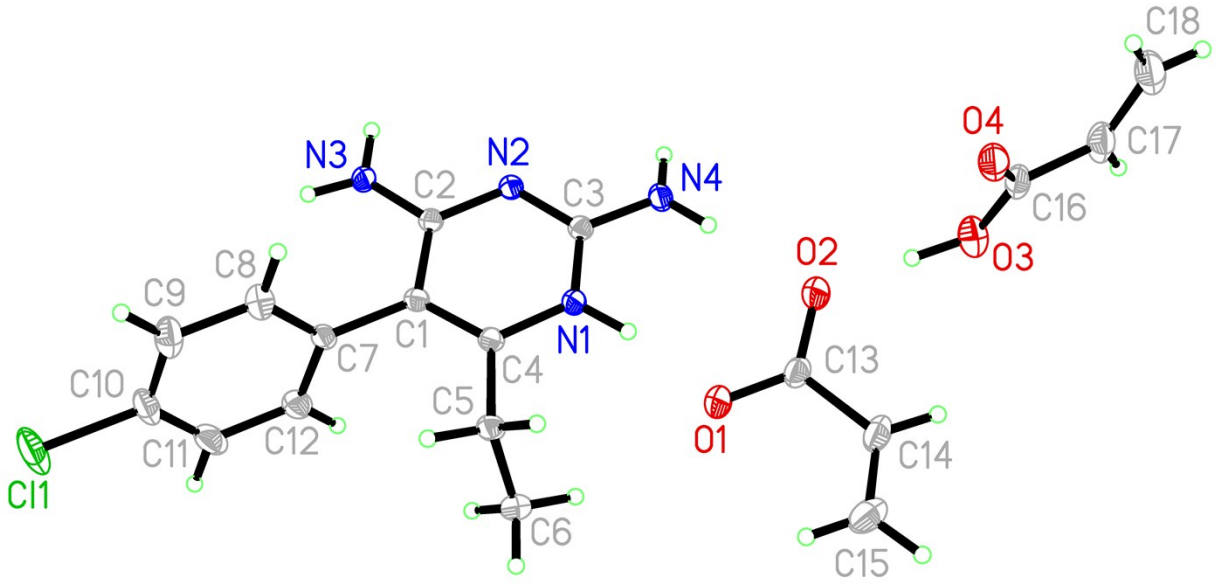

Figure S20. Illustration of asymmetric unit in PYRACR.

Structure solution and refinement. The structure was solved using SHELXT-2014/6 (Sheldrick, 2014)[6] and refined using SHELXL-2014/6 (Sheldrick, 2014).[6] The space group *P*-1 was determined based on systematic absences and intensity statistics. A direct-methods solution was calculated which provided most non-hydrogen atoms from the E-map. Full-matrix least squares / difference Fourier cycles were performed which located the remaining non-hydrogen atoms. All non-hydrogen atoms were refined with anisotropic displacement parameters. All hydrogen atoms were placed in ideal positions and refined as riding atoms with relative isotropic displacement parameters. The final full matrix least squares refinement converged to $R1 = 0.0415$ and $wR2 = 0.1010$ (F^2, obs. data).

Structure description. The structure is different than the one suggested. There are two acrylic acid molecules per pyrimethamine molecule and no solvent of crystallization. One acrylic acid molecule transfers its proton to N_1 to form a cation-anion pair. The second acrylic acid molecule acts as a hydrogen donor from O_3 to O_2 of the acrylate anion, also backed by a second hydrogen bond to form a $R_2^2(8)$ ring system.

Data collection and structure solution were conducted at the X-Ray Crystallographic Laboratory, 192 Kolthoff Hall, Department of Chemistry, University of Minnesota. All calculations were performed using Pentium computers using the current SHELXTL suite of programs. The Bruker-AXS D8 Venture diffractometer was purchased through a grant from NSF/MRI (#1229400) and the University of Minnesota.

Table S5. Crystal data and structure refinement for PYRACR.

Identification code	PYRACR	
Empirical formula	$C_{18}H_{21}ClN_4O_4$	
Formula weight	392.84	
Temperature	100(2) K	
Wavelength	0.71073 Å	
Crystal system	triclinic	
Space group	*P*-1	
Unit cell dimensions	*a* = 6.6312(4) Å	α = 97.657(2)°
	b = 12.1271(7) Å	β = 95.471(2)°
	c = 12.3925(7) Å	γ = 102.874(2)°
Volume	954.76(10) $Å^3$	
Z	2	
Density (calculated)	1.366 mg/m^3	
Absorption coefficient	0.232 mm^{-1}	
F(000)	412	
Crystal color, morphology	Colorless, Needle	
Crystal size	0.200 x 0.150 x 0.140 mm^3	
Theta range for data collection	2.602 to 30.574°	
Index ranges	$-9 \le h \le 9$, $-17 \le h \le 17$, $-17 \le h \le 17$	
Reflections collected	15122	
Independent reflections	5797 [*R*(int) = 0.0263]	
Observed reflections	4775	
Completeness to theta = 25.242°	99.7%	
Absorption correction	multi-scan	
Max. and min. transmission	0.7461 and 0.6770	
Refinement method	Full-matrix least squares on F^2	
Data / restraints / parameters	5797 / 0 / 264	
Goodness-of-fit on F^2	1.008	
Final *R* indices [*I*>2sigma(*I*)]	*R*1 = 0.0415, *wR*2 = 0.1010	
R indices (all data)	*R*1 = 0.0528, *wR*2 = 0.1108	
Largest diff. peak and hole	0.646 and -0.743 e.$Å^{-3}$	

Table S6. Atomic coordinates (x 10^4) and equivalent isotropic displacement parameters ($Å^2$x 10^3) for PYRACR. U_{eq} is defined as one third of the trace of the orthogonalized U_{ij} tensor.

	x	y	zU_{eq}	
C1	8012(2)	7164(1)	6562(1)	14(1)
C2	8768(2)	6324(1)	5890(1)	15(1)
N2	7816(2)	5831(1)	4875(1)	15(1)
C3	6097(2)	6136(1)	4505(1)	15(1)
N1	5281(2)	6902(1)	5113(1)	16(1)
C4	6231(2)	7422(1)	6142(1)	15(1)
N3	10466(2)	6006(1)	6262(1)	18(1)
N4	5099(2)	5670(1)	3505(1)	18(1)
C5	5202(2)	8269(1)	6720(1)	19(1)
C6	5744(2)	9424(1)	6321(1)	26(1)
C7	9155(2)	7710(1)	7663(1)	16(1)
C8	8907(2)	7149(1)	8568(1)	23(1)
C9	9990(2)	7651(1)	9598(1)	27(1)
C10	11326(2)	8722(1)	9706(1)	27(1)
C11	11613(2)	9301(1)	8825(1)	28(1)
C12	10523(2)	8787(1)	7800(1)	22(1)
Cl1	12688(1)	9348(1)	10993(1)	44(1)
O1	2160(2)	7718(1)	4304(1)	27(1)
O2	1253(1)	6371(1)	2820(1)	25(1)
C13	1014(2)	7253(1)	3434(1)	20(1)
C14	-780(2)	7742(1)	3076(1)	25(1)
C15	-1355(2)	8545(1)	3716(1)	30(1)
O3	-1087(2)	5453(1)	1080(1)	30(1)
O4	-3287(2)	4193(1)	1850(1)	26(1)
C16	-2632(2)	4561(1)	1042(1)	23(1)
C17	-3504(2)	4026(1)	-110(1)	30(1)
C18	-4828(2)	3024(2)	-337(1)	36(1)

Table S7. Bond lengths [Å] and angles [°] for PYRACR.

C1-C4	1.3619(15)	C8-H8	0.9500
C1-C2	1.4362(15)	C9-C10	1.381(2)
C1-C7	1.4875(15)	C9-H9	0.9500
C2-N3	1.3306(14)	C10-C11	1.380(2)
C2-N2	1.3483(14)	C10-Cl1	1.7412(13)
N2-C3	1.3342(14)	C11-C12	1.3928(18)
C3-N4	1.3349(14)	C11-H11	0.9500
C3-N1	1.3564(14)	C12-H12	0.9500
N1-C4	1.3694(14)	O1-C13	1.2453(15)
N1-H2A	0.952(19)	O2-C13	1.2763(16)
C4-C5	1.4979(15)	C13-C14	1.4992(17)
N3-H3A	0.879(17)	C14-C15	1.320(2)
N3-H3B	0.893(17)	C14-H14	0.9500
N4-H4A	0.860(17)	C15-H15A	0.9500
N4-H4B	0.908(17)	C15-H15B	0.9500
C5-C6	1.5266(18)	O3-C16	1.3062(17)
C5-H5A	0.9900	O3-H3C	0.995(19)
C5-H5B	0.9900	O4-C16	1.2269(17)
C6-H6A	0.9800	C16-C17	1.4907(17)
C6-H6B	0.9800	C17-C18	1.308(2)
C6-H6C	0.9800	C17-H17	0.9500
C7-C8	1.3922(17)	C18-H18A	0.9500
C7-C12	1.3932(16)	C18-H18B	0.9500

C4-C1-C2	116.91(10)	C3-N1-C4	120.82(10)
C4-C1-C7	122.75(10)	C3-N1-H2A	118.9(11)
C2-C1-C7	120.33(10)	C4-N1-H2A	120.1(11)
N3-C2-N2	117.52(10)	C1-C4-N1	119.64(10)
N3-C2-C1	120.12(10)	C1-C4-C5	124.67(10)
N2-C2-C1	122.36(10)	N1-C4-C5	115.68(10)
C3-N2-C2	117.73(9)	C2-N3-H3A	120.8(11)
N2-C3-N4	119.91(10)	C2-N3-H3B	121.5(10)
N2-C3-N1	122.50(10)	H3A-N3-H3B	116.5(15)
N4-C3-N1	117.58(10)	C3-N4-H4A	117.7(11)

C3-N4-H4B	118.3(10)	C10-C11-C12	118.85(12)
H4A-N4-H4B	123.9(15)	C10-C11-H11	120.6
C4-C5-C6	111.76(10)	C12-C11-H11	120.6
C4-C5-H5A	109.3	C11-C12-C7	120.75(12)
C6-C5-H5A	109.3	C11-C12-H12	119.6
C4-C5-H5B	109.3	C7-C12-H12	119.6
C6-C5-H5B	109.3	O1-C13-O2	124.17(11)
H5A-C5-H5B	107.9	O1-C13-C14	118.68(12)
C5-C6-H6A	109.5	O2-C13-C14	117.15(11)
C5-C6-H6B	109.5	C15-C14-C13	122.29(13)
H6A-C6-H6B	109.5	C15-C14-H14	118.9
C5-C6-H6C	109.5	C13-C14-H14	118.9
H6A-C6-H6C	109.5	C14-C15-H15A	120.0
H6B-C6-H6C	109.5	C14-C15-H15B	120.0
C8-C7-C12	118.87(11)	H15A-C15-H15B	120.0
C8-C7-C1	120.78(10)	C16-O3-H3C	115.6(11)
C12-C7-C1	120.34(11)	O4-C16-O3	124.64(12)
C7-C8-C9	120.99(12)	O4-C16-C17	123.58(13)
C7-C8-H8	119.5	O3-C16-C17	111.78(12)
C9-C8-H8	119.5	C18-C17-C16	121.68(15)
C10-C9-C8	118.66(13)	C18-C17-H17	119.2
C10-C9-H9	120.7	C16-C17-H17	119.2
C8-C9-H9	120.7	C17-C18-H18A	120.0
C11-C10-C9	121.88(12)	C17-C18-H18B	120.0
C11-C10-Cl1	119.45(11)	H18A-C18-H18B	120.0
C9-C10-Cl1	118.67(11)		

Symmetry transformations used to generate equivalent atoms:

Table S8. Anisotropic displacement parameters ($Å^2 x\ 10^3$) for PYRACR. The anisotropic displacement factor exponent takes the form: $-2\pi^2[\ h^2\ a^{*2}U_{11} + ...\ + 2\ h\ k\ a^*\ b^*\ U_{12}\ ]$

	U_{11}	U_{22}	U_{33}	U_{23}	U_{13}	U_{12}
C1	14(1)	13(1)	16(1)	1(1)	1(1)	4(1)
C2	14(1)	13(1)	16(1)	2(1)	1(1)	3(1)
N2	15(1)	15(1)	16(1)	0(1)	0(1)	6(1)
C3	14(1)	13(1)	16(1)	2(1)	1(1)	3(1)
N1	14(1)	16(1)	17(1)	-1(1)	-1(1)	6(1)
C4	15(1)	13(1)	16(1)	1(1)	2(1)	3(1)
N3	19(1)	19(1)	17(1)	-1(1)	-2(1)	10(1)
N4	16(1)	20(1)	17(1)	-2(1)	-2(1)	6(1)
C5	17(1)	19(1)	21(1)	-3(1)	0(1)	8(1)
C6	33(1)	19(1)	26(1)	0(1)	-1(1)	12(1)
C7	14(1)	16(1)	17(1)	-2(1)	0(1)	6(1)
C8	21(1)	26(1)	20(1)	3(1)	0(1)	3(1)
C9	26(1)	40(1)	17(1)	2(1)	1(1)	11(1)
C10	20(1)	37(1)	21(1)	-12(1)	-6(1)	13(1)
C11	23(1)	22(1)	34(1)	-9(1)	-6(1)	3(1)
C12	20(1)	19(1)	26(1)	0(1)	-1(1)	3(1)
Cl1	34(1)	63(1)	28(1)	-24(1)	-14(1)	22(1)
O1	22(1)	27(1)	30(1)	-2(1)	-8(1)	10(1)
O2	20(1)	26(1)	27(1)	0(1)	-4(1)	8(1)
C13	15(1)	21(1)	25(1)	6(1)	-1(1)	5(1)
C14	18(1)	28(1)	30(1)	10(1)	-2(1)	7(1)
C15	23(1)	26(1)	45(1)	12(1)	4(1)	10(1)
O3	27(1)	38(1)	22(1)	2(1)	-2(1)	5(1)
O4	22(1)	30(1)	23(1)	-1(1)	-1(1)	8(1)
C16	20(1)	30(1)	19(1)	-3(1)	-3(1)	13(1)
C17	27(1)	41(1)	20(1)	-4(1)	-5(1)	15(1)
C18	26(1)	45(1)	32(1)	-10(1)	-6(1)	13(1)

Table S9. Hydrogen coordinates (x 10^4) and isotropic displacement parameters (Å^2 x 10^3) for PYRACR.

	x	y	z	U(eq)
H2A	4080(30)	7106(16)	4799(15)	36(5)
H3A	10870(30)	5447(14)	5884(13)	22
H3B	11080(30)	6243(14)	6953(14)	22
H4A	5660(30)	5220(14)	3101(14)	22
H4B	3900(30)	5868(14)	3282(13)	22
H5A	5652	8378	7520	23
H5B	3671	7963	6593	23
H6A	5034	9953	6710	39
H6B	5290	9321	5530	39
H6C	7256	9741	6466	39
H8	7985	6412	8482	27
H9	9814	7265	10213	33
H11	12538	10037	8917	34
H12	10715	9175	7186	27
H14	-1530	7464	2364	30
H15A	-623	8834	4431	36
H15B	-2500	8835	3463	36
H3C	-300(30)	5777(16)	1820(16)	36
H17	-3087	4422	-694	36
H18A	-5257	2619	239	43
H18B	-5360	2702	-1079	43

Table S10. Torsion angles [°] for PYRACR.

C4-C1-C2-N3	-178.06(10)	C4-C1-C7-C12	-81.85(15)
C7-C1-C2-N3	1.85(16)	C2-C1-C7-C12	98.25(13)
C4-C1-C2-N2	2.02(16)	C12-C7-C8-C9	0.44(19)
C7-C1-C2-N2	-178.08(10)	C4-C1-C7-8	99.30(14)
N3-C2-N2-C3	179.12(10)	C2-C1-C7-C8	-80.60(14)
C1-C2-N2-C3	-0.95(16)	C1-C7-C8-C9	179.30(11)
C2-N2-C3-N4	-179.92(10)	C7-C8-C9-C10	-0.1(2)
C2-N2-C3-N1	-0.81(16)	C8-C9-C10C11	-0.1(2)
N2-C3-N1-C4	1.47(17)	C8-C9-C10-Cl1	-179.78(10)
N4-C3-N1-C4	-179.41(10)	C9-C10-C11-C12	-0.1(2)
C2-C1-C4-N1	-1.34(16)	Cl1-C10-C11-C12	179.63(10)
C7-C1-C4-N1	178.76(10)	C10-C11-C12-C7	0.4(2)
C2-C1-C4-C5	179.73(10)	C8-C7-C12-C11	-0.60(18)
C7-C1-C4-C5	-0.17(18)	C1-C7-C12-C11	-179.46(11)
C3-N1-C4-C1	-0.29(16)	O1-C13-C14-C15	-9.2(2)
C3-N1-C4-C5	178.73(10)	O2-C13-C14-C15	170.19(13)
C1-C4-C5-C6	99.30(14)	O4-C16-C17-C18	-10.4(2)
N1-C4-C5-C6	-79.66(13)	O3-C16-C17-C18	168.9

Table S11. Hydrogen bonds for PYRACR [Å and °].

D-H...A	d(D-H)	d(H...A)	d(D...A)	<(DHA)
N1-H2A...O1	0.952(19)	1.712(19)	2.6550(13)	169.8(17)
N3-H3A...N2#1	0.879(17)	2.101(17)	2.9747(14)	172.8(15)
N3-H3B...O4#2	0.893(17)	2.183(17)	2.9244(14)	140.1(14)
N4-H4A...O4#3	0.860(17)	2.126(17)	2.9751(14)	169.1(15)
N4-H4B...O2	0.908(17)	2.041(17)	2.9484(14)	177.9(15)
O3-H3C...O2	0.995(19)	1.517(19)	2.5000(14)	168.5(18)

Symmetry transformations used to generate equivalent atoms:

#1 -x+2,-y+1,-z+1 #2 -x+1,-y+1,-z+1 #3 x+1,y,z

1. Hartmann SR, Hahn EL, Nuclear double resonance in the rotating frame. *Phys Rev* 128(5), 2042–2053, (1962).

2. Fung BM, Khitrin AK, Ermolaev K, An improved broadband decoupling sequence for liquid crystals and solids. *J Magn Reson,* 142, 97–101, (2000).

3. APEX2, Bruker Analytical X-ray Systems, Madison, WI (2014).

4. SADABS, Bruker Analytical X-ray Systems, Madison, WI (2014).

5. SAINT Bruker Analytical X-ray Systems, Madison, WI (2014).

6. SHELXTL 2013, Bruker Analytical X-Ray Systems, Madison, WI (2013); G. M. Sheldrick, *Acta Cryst.* **A64**, 112-122 (2008).